

Electron-metal-surface interaction potential with vacuum tunneling: Observation of the image force

G. Binnig, N. García, and H. Rohrer

Zurich Research Laboratory, International Business Machines Corporation,
CH-8803 Rüschlikon, Switzerland

J. M. Soler and F. Flores

División de Física, Universidad Autónoma de Madrid,
Cantoblanco, Madrid 34, Spain

(Received 22 May 1984)

It is shown that the classical image potential plays an important role in the correct interpretation of vacuum-tunneling experiments. The logarithmic derivative of the tunnel current with respect to the electrode separation is nearly constant and approximately equal to the square root of the average work function. From the experimental tunnel-voltage dependence with the electrode separation we obtain the barrier height as a function of distance.

One of the fundamental problems in surface physics is obtaining knowledge of the electron-metal-surface interaction potential.¹ It is generally accepted that at large distances from the surface, the electron "feels" the classical image that varies as $1/(z - z_0)$ where z is the normal coordinate of the electron to the surface, and z_0 the position of the image plane. But before the electron position reaches z_0 , the potential has to saturate to the value of the bottom of the metal conduction band. It has been assumed that within the density-functional theory² for a jellium model describing the metal, the electron potential saturates to the local density exchange and correlation potential.³

Electron tunneling probes this interaction potential since the electron "sees" the superposition of the two surface barriers between which the tunneling takes place. The problem is simplified when the tunneling time is long compared to the rearrangement time of the surface charges. According to a recent theory by Büttiker and Landauer⁴ that does not consider many-body effects, this should generally be the case. In turn, experimental verification of this "static" interaction potential would confirm this relative time scale of the tunnel process. It is the purpose of this Brief Report to present evidence for the presence of the image potential in vacuum-tunneling experiments. Our findings are crucial to the application of scanning tunneling microscopy to surface chemistry.

The image potential will have a significant effect on the tunnel resistance at barrier widths below 15 Å. In an experiment by Weinberg and Hartstein,⁵ a large voltage was applied to a tunnel junction of some 1000-Å electrode separation, thus quenching the active tunnel barrier to a sufficiently small width. They concluded that image forces are absent. The scanning tunneling microscopy recently developed offers an alternate possibility.⁶ There, the tunnel barrier is a vacuum gap between two electrodes, the width of which can be controlled within 0.1 Å. A significant advantage of this technique is also the bare electrode surfaces. Also there are recent indications by Puri and Schaich⁴ claiming that the model of Ref. 5 is unwarranted.

The potential from the images and counter-images created by the electron on the two plane surfaces is approximately

given by

$$V_{\text{im}}(z) \approx -\frac{e^2}{d} \left[(\ln 2 - 1) + \left(\frac{z}{d} \right)^2 + \frac{1}{1 - 4(z/d)^2} \right], \quad (1)$$

where $d = s - 1.5$ Å is the distance between image planes, s the distance between the jelliums, as indicated by Lang and Kohn,³ and z is measured from the middle point of the two surfaces. In Fig. 1, we present the form of this potential plus the electrostatic potential, V_{el} , resulting from integrating Poisson's equation for the density profile $n(z)$ also indicated in the same figure. We used the profile of Smith⁷ with an exponential decay in the density that gives good agreement with atom surface scattering.⁸ The calculations were made for an Au-W tunnel junction having Fermi energies and work functions of 5.5 and 5.2 eV, and 8.0 and 4.5 eV, for Au and W, respectively. Notice that the image force potential diverges at the image planes corresponding to $z = \pm 2.25$ Å in the figure.

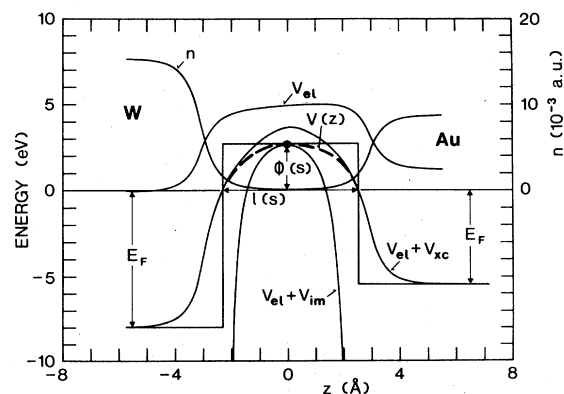


FIG. 1. Electron density $n(z)$ and various potentials for a W-Au vacuum tunnel junction with $s = 6$ Å. $V_{\text{el}}(z)$, electrostatic potential; $V_{\text{im}}(z)$, image potential; $V_{\text{xc}}(z)$, local exchange and correlation potential; $V(z)$, tunnel barrier; $\phi(s)$ and $l(s)$, height and width, respectively, of approximate square tunnel barrier.

The actual potential, $V(z)$, has to approach $V_{el} + V_{xc}$, where V_{xc} is the local exchange and correlation potential, close to the jellium and approach $V_{el} + V_{im}$ away from it. Matching was done at the Fermi level and in the middle of the gap. The resulting $V(z)$ is flat at the top and for the following is replaced by a rectangular barrier of height $\phi(s)$ and width $l(s)$. Detailed calculations using the approach of Ref. 9 show that this is a good approximation, which furthermore does not depend strongly on the interpolation used for matching $V(z)$. Physically, the approximation by the square barrier is a trade off of enhanced and reduced tunnel probabilities. The dominant contribution to the tunnel current comes from electrons tunneling at about 20° – 30° from the surface normal for which $E_{kin,z} < E_F$.^{9,10} For a square barrier, these electrons “see” a larger average barrier height but a smaller barrier width. We further find that $l(s) = s - 1.4 \text{ \AA}$, i.e., $l(s) \approx d$, thus

$$\phi(d) = \phi_0 - \frac{\alpha}{d}, \quad (2)$$

where ϕ_0 is the average work function and $\alpha \approx 9.97 \text{ eV \AA}$. It has been shown that for a square barrier, the tunnel current I from a tip of radius R to a plane metal surface (the configuration used in the present experiments), is given approximately by using the interpolation formula⁹

$$I(s) \approx \frac{\hbar e}{2m} N(E_F) G(R) \exp[-2\phi^{1/2}l(s)], \quad (3)$$

where $G(R)$ is a geometrical factor⁹ depending on the tip radius R , $N(E_F)$ the density of states at the Fermi level of the negative electrode, V the applied voltage, and $\phi_{\text{eff}} = (1 + \beta)\phi(s)$. The parameter β accounts for the fact that the average barrier height is larger than $\phi(s)$. For a planar junction, $\beta \approx 0.32$ and for a tip radius of 5 \AA , $\beta \approx 0.15$.⁹ The strong s dependence of $\phi(s)$ is expected to have a significant effect on the s dependence of the tunnel current. Notice that $\phi(s) = \phi_0 - \alpha/(s - 1.5)$. Also, we have used Eq. (3) for a qualitative discussion, but in all our results (Fig. 3) we have used the exact numerical calculations for the model of Fig. 1.

Surprisingly enough, the experiments¹¹ show a straight line for the logarithmic derivative of $I(s)$, with a slope close to $\phi^{1/2}$. Although at that time, the absolute electrode separation was undetermined, we now⁶ know that it was well within the range where the image potential plays a role. We have made new experiments with a W tip and a flat Au(100) surface, working in the current-stabilized mode. Instead of measuring $I(s)$ at constant V , we determined $V(s)$ at constant I , obtaining information on the local electron-surface interaction potential. In this procedure, thermal drifts can easily be eliminated. As shown in Fig. 2, we again find a straight line of $\ln(1/V)$ vs s . Finally, $d(\ln I)/ds$, measured directly with the modulation technique,⁶ was also nearly independent of the applied voltage and thus of s .

In the following, we show that these experiments [$d(\ln I)/ds \approx \text{const}$, $\phi \approx \phi_0$] do not indicate the absence of an image potential but are fully consistent with its existence.

Taking a square barrier of height $\phi(d)$ given by Eq. (2), one easily finds

$$\frac{d(\ln I)}{ds} = 2\phi^{1/2} \left[1 + \frac{\alpha^2}{8\phi\beta d^2} + O\left(\frac{1}{d^3}\right) \right] (1 + \beta). \quad (4)$$

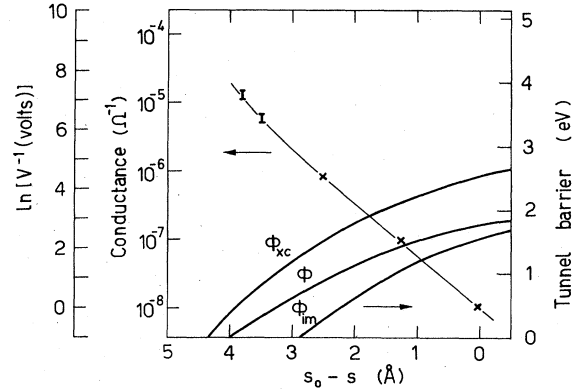


FIG. 2. Experimental decrease of tunnel-gap width s as a function of applied voltage, V , at constant tunnel current $I = 10 \text{ nA}$. Thermal voltages across the tunnel junctions give the uncertainty in voltage indicated by the error bars. The slope yields an effective barrier height of $\phi_0 = 3.2 \text{ eV}$. Total barrier, ϕ , image barrier, ϕ_{im} , and exchange-correlation barrier, ϕ_{xc} , are shown in eV in the right ordinate.

Thus, the first-order term in $1/d$, although present in $\phi(d)$, cancels exactly for the slope of $I(s)$. Figure 3 shows the results of numerical calculations of the tunnel conductance, σ , for a square barrier as a function of s with $\phi_0 = 4.8 \text{ eV}$. In the distance range considered, no appreciable deviation from a straight line appears for a planar junction, although the average barrier height decreases from 4 eV to nearly zero. For a tip-plane junction, σ increases even faster for small s , exactly as observed. (This bending upwards moves to larger s as ϕ_0 decreases.) This is not merely the consequence of adopting a square barrier as can be seen from the continuous line which is a numerical integration of the Schrödinger equation for a barrier of shape $V(z)$ and planar electrodes. Also, a straight line appears but with a slope 17% smaller. This is the effect of taking the averaged tun-

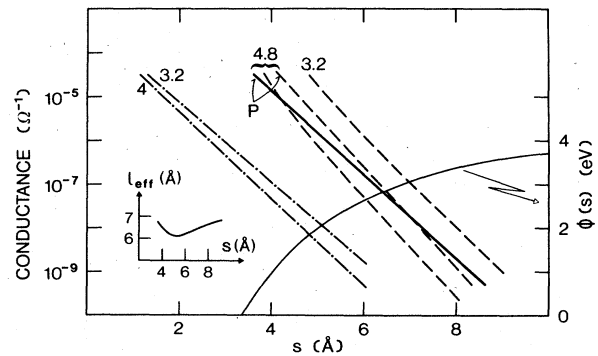


FIG. 3. Calculated conductances as a function of electrode separation for a barrier height $\phi(s)$ and a spherical tip of radius $R = 5 \text{ \AA}$ (the two curves denoted by P are for planar junctions of area πR^2). The numbers with the curves give the values of ϕ_0 used. Dashed curves, $\phi(s)$ according to Eq. (2); dashed-dotted, $\phi(s) = \text{const} = \phi_0$; solid line, “real” barrier $V(z)$. Notice the increase in conductance by considering the image potential. Also given is $\phi(s)$ for $\phi_0 = 4.8$. The inset shows the lateral resolution l_{eff} of the scanning tunneling microscope for a tip radius of 5 \AA .

nel barrier. Notice that at a small distance of 3.5 Å, the square barrier overestimates the conductance by a factor of 3, and the opposite happens by a factor of 1.5 at 9 Å. However, the effect of the distance-dependent barrier height clearly shows up in the absolute values of the conductance. With a constant barrier height of 3.2 eV corresponding to the measured slope, we obtain with Eq. (3), $s_0 = 5.7$ Å for the lowest-conductance σ measured (see Fig. 3). However, the barrier must collapse at $d \approx 1.5$ Å ($s \approx 3$ Å) since there, the electron densities at the Fermi-level touch and metallic conduction with $\sigma \approx 10^{-2} \Omega^{-1}$ sets in. But at $s_0 = 3.8$ Å ($s = 1.9$ Å) we still observe a conductance of $\sigma \approx 10^{-5} \Omega^{-1}$. Thus, the barrier height has to vary substantially in the range of the experiment. Such an s -dependent barrier height can only yield a constant slope of I vs s if it varies according to Eq. (2), i.e., the barrier is lowered by the image potential.

Moreover, from experiments of Fig. 2 and Eq. (3) we can calculate $\phi(s)$ by noting that for $s \rightarrow \infty$, $\phi_{\text{eff}}(s) \rightarrow 1.15[\phi_0 - (\alpha/d)]$, and by taking into account that for $s_0 - s = 4$ Å, $\phi_{\text{eff}} \approx 0$, because we have an experimental contact point. From these conditions we obtain (i) the barrier potential given in Fig. 2 and (ii) $s_0 = 7.4$ Å, the barrier collapsing at $s \approx 3.4$ Å. In the same figure, we show the barrier potentials due to the exchange correlation, V_{xc} , and image effects, V_{im} . Our results tend to saturate to the image potential at long distances and to the exchange-correlation potential at close contact.

Finally, we make three remarks. The resolution of the tunneling microscope is predicted to decrease with increasing gap width^{9,12} and decreasing barrier height although

Tersoff and Hamann¹² do not take the image potential into account. As an effect of the image potential, the resolution goes through a broad maximum at $s \approx 5$ Å as shown in the inset of Fig. 3. This is in accordance with experiments which do not show a substantial change of resolution in the 4 to 10 Å range. Second, the effect of tip and surface geometry on the image potential has been neglected, but we do not expect this to affect the present results substantially. However, recent experiments showed that surface roughness (and thus also very small tip radii) can drastically reduce the overall barrier height, independent of the image potential. This is believed to be the reason for the reduced ϕ_0 observed in the present experiment, and is planned to be the subject of a future paper. Third, Dose¹³ has recently observed with inverse photoemission, the empty hydrogenic band states localized in the image potential of Cu(100), confirming our observations.¹⁴

In summary, we have shown that the "static" image potential is necessary to describe correctly the barrier-width dependence and absolute value of the vacuum tunnel current. On the other hand, the logarithmic derivative of the tunnel current is nearly independent of the electrode separation, and is determined by the barrier height at large distances. This is an important result for application of scanning tunneling microscopy to surface chemistry because $d \ln I / ds$ is a direct measure of the work function irrespective of the tip-surface distance.

We thank Ch. Gerber for diligent assistance in the experiments, A. Baratoff and E. Stoll for valuable discussions, and V. Dose for communicating his results prior to publication.

¹D. Lang, *Solid State Phys.* **28**, 225 (1973), and references therein.

²N. D. Lang and W. Kohn, *Phys. Rev. B* **1**, 4555 (1970).

³N. D. Lang and W. Kohn, *Phys. Rev. B* **3**, 1215 (1971).

⁴M. Büttiker and R. Landauer, *Phys. Rev. Lett.* **49**, 1739 (1982); A. Puri and W. L. Schaich, *Phys. Rev. B* **28**, 1781 (1983).

⁵Z. A. Weinberg and A. Hartstein, *Solid State Commun.* **20**, 179 (1976).

⁶For references, see G. Binnig and H. Rohrer, *Helv. Phys. Acta* **55**, 726 (1983); *Surf. Sci.* **126**, 236 (1983).

⁷J. R. Smith, *Phys. Rev.* **181**, 522 (1969).

⁸N. García, J. A. Barker, and I. P. Batra, *J. Electron Spectrosc. Relat. Phenom.* **30**, 137 (1983); *Solid State Commun.* **47**, 485 (1983).

⁹N. García, C. Ocal, and F. Flores, *Phys. Rev. Lett.* **50**, 2002 (1983).

¹⁰G. Beuermann, *Verh. Dtsch. Phys. Ges.* **18**, 1031 (1983).

¹¹G. Binnig, H. Rohrer, Ch. Gerber, and E. Weibel, *Appl. Phys. Lett.* **40**, 178 (1982).

¹²J. Tersoff and D. R. Hamann, *Phys. Rev. Lett.* **50**, 1999 (1983).

¹³V. Dose *et al.*, *Phys. Rev. Lett.* **52**, 1919 (1984); (private communication). Also D. Straub and F. J. Himpsel [*Phys. Rev. Lett.* **52**, 1922 (1984)] have observed image states in Cu(100) and Au(100).

¹⁴B. Reihl, K. H. Frank, and R. R. Schlittler (unpublished) have also observed image states in Ag(100).